Journal of Physics: Conference Series **2586** (2023) 012075 doi:10.1088/1742-6596/2586/1/012075

Fission fragment mass distribution of ^{187}Ir

Sangeeta Dhuri[1,2], K. Mahata[1,2], A. Shrivastava[1,2], K. Ramachandran[1], S. K. Pandit[1], Vineet Kumar[1], V. V. Parkar[1,2], P. C. Rout[1,2], A. Kumar[1], Arati Chavan[3], Satbir Kaur[1,2], T. Santhosh[1,2]

[1]Nuclear Physics Division, Bhabha Atomic Research Centre, Mumbai - 400085, India
[2]Homi Bhabha National Institute, Anushaktinagar, Mumbai - 400094, India
[3]Vivekanand Education Society's College of Arts, Science and Commerce, Mumbai - 400071, India

E-mail: sangdhuri2011@gmail.com

Abstract. The fission fragment mass and total kinetic energy (TKE) distributions were studied for ^{187}Ir populated using ^{12}C + ^{175}Lu reaction at excitation energies 24.8, 23.3, 20.8, and 16.7 MeV above the saddle point. Fission fragments (FF) were detected using position sensitive MWPC's kept at a folding angle. The mass of the fragment was calculated using Time-of-Flight (TOF) difference method. The multi Gaussian fit to the extracted mass distributions shows the presence of narrower microscopic components corresponding to Z = 38 and 45 in addition to the liquid drop component at lower excitation energies. The GEF model predicts significant asymmetric components at all the measured energies. The TKE distribution investigations suggest the dominance of macroscopic liquid drop components at all energies.

1. Introduction

Being one of the most dramatic examples of nuclear decay, the nuclear fission phenomenon continues to be a puzzle for many reasons since its discovery. Nevertheless, the nuclear fission phenomenon in actinides is well explored both theoretically and experimentally. The strong shell effects corresponding to Z = 52 (S1 mode) and Z = 54 (S2 mode) of the fragments are identified to be driving force of asymmetry along with so called super-long modes in this region. In the pre-actinide region, the data is scarce because of low fission probabilities leading to less statistics at low energies where the shell effects are most effective. Though a slight dip or flattning at the center of the mass distribution was observed for nuclei with A $\sim$ 200 in p and α induced reactions, the mass distribution for the nuclei on either sides were dominantly symmetric, considered to be driven by macroscopic liquid drop [1, 2, 3]. The dominent asymmetric split was observed in case of β-delayed fission of ^{180}Tl [4] instead of most anticipated symmetric mass split because of semi-magic ^{90}Zr. This unexpected asymmetric split ($A_L = 80$, $A_H = 100$) has generated lot of interest in this region both theoretically and experimentally. Because of the restrictions such as Q values of the reactions, lower statistics, only limited systems can be studied using β-delayed fission in this region. Hence, the heavy ion induced fusion fission reaction channels were explored to probe the asymmetric fission phenomenon. On the theoretical front, calculations using various models namely BSM [5], ISP model [6], Microscopic energy density functional(EDF) calculations [7], semi empirical GEF model [8] were performed to understand the nature of the mass split in this mass region and gave different interpretations. As per BSM, the large shell gaps at neutron

number N = 108 of ^{186}Pt is responsible for asymmetric saddle point which is responsible for the asymmetric mass split. It is in qualitative agreement with the experimentally observed mass asymmetry in nuclei near ^{180}Hg. A recent systematic study has proposed the dominance of proton shells ($Z \approx 36$) [9] in the light fragment in deciding the asymmetric split in the pre-actinde region. This observation was further substantiated by the calculation based on the microscopic EDF framework, which shows shell gaps at $Z = 34$ and 38 for $N < 50$ and N $\geq$ 50. Thus more measurements are required to differentiate between various theoretical interpretations

In the present study, the fission fragment mass and total kinetic energy (TKE) distributions are studied for ^{187}Ir nucleus at various excitation energies. ^{187}Ir lies at the central region of the the island of asymmetry predicted by the BSM model [10], whereas it has 2 $\times$ (Z $\approx$ 38, N $\approx$ 56) shell configuration adding symmetric component which are otherwise considered to catalyse the asymmetric split in case of pre-actinides.

2. Experimental Details and Data Analysis

The experiment was performed at the BARC-TIFR PLF, Mumbai. The bunched beam of ^{12}C bombarded on a ^{175}Lu target (250 μg/cm^2 thick on 170 μg/cm^2 thick Al backing). The rf - pulse repetition period was 213.4 ns with two bunches crossing each period. A BaF_2 detector was placed at the beam dump to monitor the time structure of the bunch by detecting γ-rays. The typical width (σ) of the beam bunch was 0.6 ns after deconvolution of BaF_2 timing resolution. The beam energies were 58, 65, 70 and 75 MeV corresponding to compound nuclear excitation energies 38.7, 45.2, 49.9, 54.6 MeV, respectively. The experimental fission cross section at E_{Lab} = 74.3 MeV is 1.2 mb [11] and estimated cross sections at E_{Lab} = 58 MeV is of the order of few μb from the present measurement. The time-of-flights (TOF), position (x, y) and the energy deposited by each of the fission fragments were recorded using two position-sensitive multiwire proportional chambers (MWPC). The active areas of both the detectors were 125 mm $\times$ 75 mm mounted at angles 113° and $-$50° at a distance of 24 cm from the target. The target was kept at 40° with respect to the beam direction to minimize the energy loss of the fragment in the target and backing.

The details regarding data analysis are discussed in Ref.[12]. The TOF calibration was done using the timing of elastic events information and position calibration was done using detector mask. TOF spectra from MWPC 1 vs 2 generated using the RF and cathode signal was used to separate the fission events from quasi-elastic events.(Ref.[12], Fig.1(a)). The individual velocities of the fragments were extracted using TOF and position information. The correlation plots generated for azimuthal and folding angle and the perpendicular and parallel components of the fragment velocities confirms the binary nature of the reactions (Ref. [12], Fig.1(b,c)). The preneutron mass of the fission fragments were extracted using the time difference method. The charges of individual fragments Z_1, Z_2 were estimated assuming unchanged charge density (UCD) of the compound nucleus[13]. Average energy loss by the fragments in the target and backing is estimated using SRIM[14] software using range vs E/A method on an event-by-event basis and energies as well as masses of the fragments were corrected accordingly.

3. Results and Discussions

The experimentally extracted mass distributions are shown in Fig.1(a-d). The investigations of the obtained mass distributions are done by comparing them with predictions of the GEF(Version 2021/1.1) [8] code at same excitation energies (E^*_{cn}) and $< l >_{fus}$. The predictions (total, symmetric, asymmetric) of GEF code folded with experimental mass resolution are plotted together in Fig.1(a-d). At all the E_{sad}, the GEF code predicts significant asymmetric mass division hinting at the presence of microscopic corrections to the macroscopic potential energy surface. As we go higher in excitation energy the widths are increasing accordingly. Also, the two Gaussian fittings to the asymmetric components of the GEF data give an average

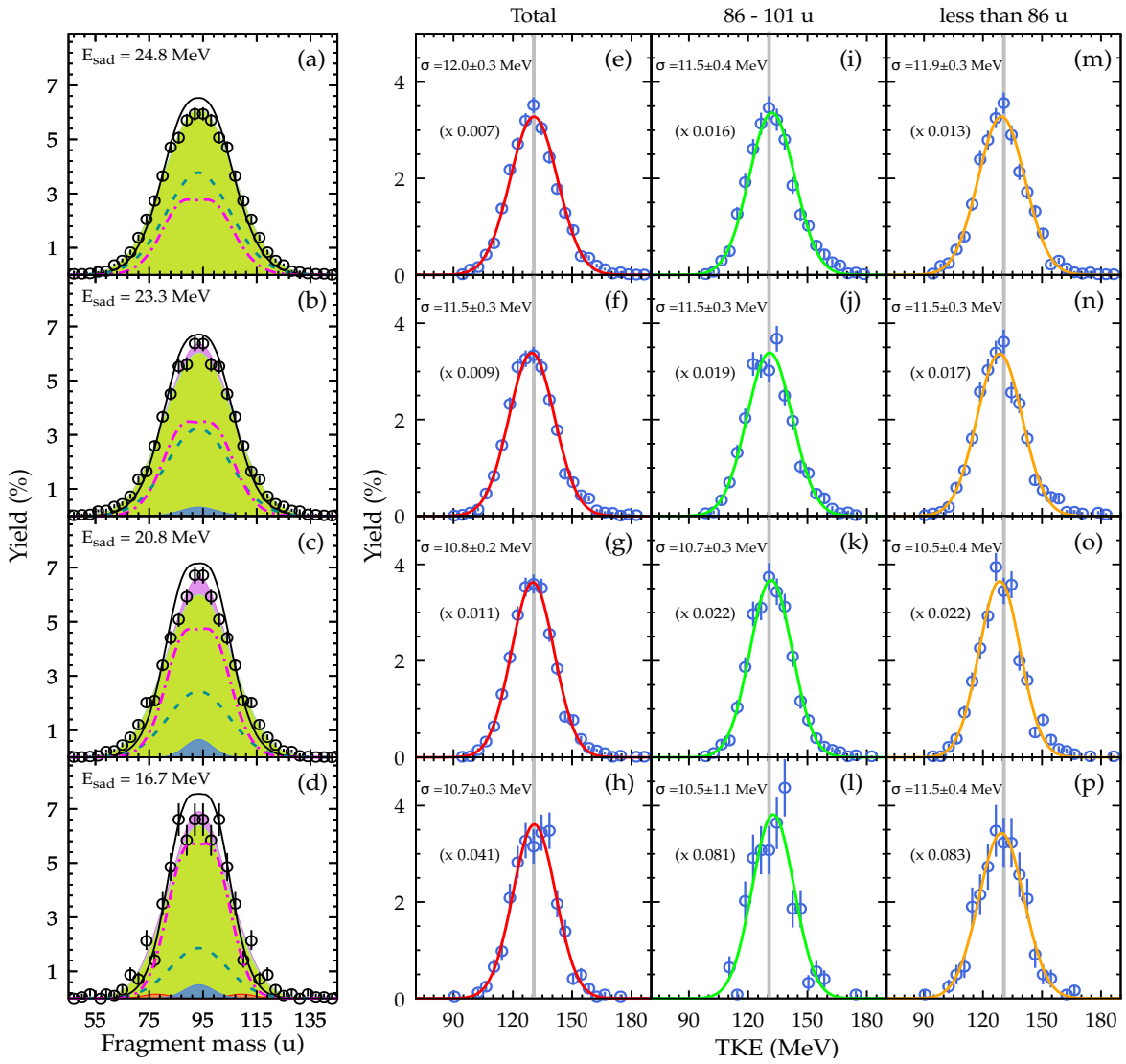

Figure 1. [Left panel]: (a-d), The experimental mass yields (open circles) along with the result of multi-Gaussian (MG) fits to the data (pink color shaded region). The different fission modes corresponding to macroscopic liquid drop component (green shaded region) together with microscopic components corresponding to $Z \approx 38$ (blue shaded region) and $Z \approx 45$ (red shaded region) shells. The solid, dashed, and dot-dashed lines represents the total, symmetric and asymmetric components predicted using GEF [8] code. [Right panel]: The first column(e-h), the TKE distributions obtained for ^{187}Ir at various E_{sad} corresponding to mass distribution spectra on left are shown. Second (i-l) and third (m-p) column, the TKE distributions obtained for different mass regions are shown. The solid lines represents the single Gaussian fit to the data and corresponding widths (σ) are mentioned. The vertical solid lines represents the expected TKE values at mean mass expected from macroscopic model [15]. The counts in all three columns are multiplied with the constant written in the brackets to normalize total yield to 100%.

position of $A_L \sim 89 (Z_L \sim 36)$. While the experimental distributions are found to be narrower at the central part, it's tail part is broader than the GEF (symmetric + asymmetric) predictions. Conversely, in an attempt of multiple Gaussian (MG) fit to the data, the contribution of

microscopic shell ($Z \approx 38$ and 45) effects are found to be small compare to the macroscopic LD contribution. As discussed in ref. [12], the theretical models predicts more substantial microscopic components than extracted from multi Gaussian fit.

Further we have studied the measured mass-TKE correlations. The sensitivity of TKE to different fission modes has been inferred in few recent studies [15, 17]. From the observed correlations of the decomposed TKE components with the fragment mass, the existence of well deformed Z $\approx$ 38 and less deformed Z $\approx$ 45 shells were concluded [15, 17]. The experimentally extracted TKE distributions for the present system are shown in Fig.1(e-h). The TKE distributions could be fitted with single Gaussian. The widths of the TKE distributions obtained from single Gaussian fit varies from 10.7 MeV to 12 MeV with increase in excitation energy. Further the analysis is extended for TKE distributions for different mass regions (Fig.1(i-p)). The mass ranges are chosen such a way that effects on TKE (or influence on TKE) due two microscopic ($Z \approx 38$ and 45) components can be studied separately. All the mass-gated TKE distributions could be describe well with single Gaussian and the TKE distributions peaked at values predicted using Viola [16] systematics. Thus for the present data indicate the dominance of LD behavior.

4. Summary

The ^{187}Ir nucleus was populated using ^{12}C + ^{175}Lu reaction at four E_{sad} energies 16.7, 20.8, 23.3, and 24.8 MeV respectively. The fission fragment mass distribution and TKE distributions were studied to investigate shell effects. The multi Gaussian fit to the mass distribution results in narrow components corresponding to $Z = 38$ and 45 compatible with the earlier observations at the lowest energies. The measured mass distributions are found to be different from theoretical description. The TKE distributions are also agreeing well with the macroscopic TKE values. The mass gated TKE distributions also peaked at the macroscopic energies corresponding to mean mass of the range selected. The TKE distribution investigations indicates dominance of macroscopic LD component.

5. Acknowledgments

The authors are thankful to the PLF staff for smooth operation of the machine and Mr. P. Patale for his help during experiment. One of the authors S. D. is sincerely grateful to Department of Science and Technology, India for financial support under the DST-INSPIRE Fellowship scheme.

6. References

[1] Itkis M. G., Okolovich V N and Rusanov A Y 1985 Z. Phys. A 320 433441,
[2] Itkis M. G., Kondratev N A and Mulgin S I 1990 Yad. Fiz. 52(4) 944959
[3] Itkis M. G., Kondratev N A, Mulgin S I, Okolovich V N, Rusanov A Y and N S G 1991 Yad. Fiz. 53 12251237
[4] Andreyev A. N. et al., 2010 Phys. Rev. Lett. 105(25) 252502
[5] Moller P., Randrup J. and Sierk A. J. 2012 Phys. Rev. C 85(2) 024306
[6] Andreev A. V., Adamian G. G. and Antonenko N. V. 2012 Phys. Rev. C 86(4) 044315
[7] Scamps G. and Simenel C. 2019 Phys. Rev. C 100(4) 041602(R)
[8] Schmidt K. H. et al., 2016 Nucl. Data Sheets 131 107221 ISSN 0090-3752 special Issue on Nucl. Reaction Data
[9] Mahata K. et al., 2022 Phys. Lett. B 825 136859 ISSN 0370-2693
[10] Moller P. and Randrup J. 2015 Phys. Rev. C 91(4) 044316
[11] Sikkeland T. el al., 1971 Phys. Rev. C 135(3B) B669
[12] Dhuri Sangeeta et al., 2022 Phys. Rev. C 106(1) 014616
[13] Vandenbosch R. and Huizenga J. 1973 Nuclear fission (Academic,New York)
[14] Ziegler J. F. at al., 2010 Nucl. Instrum. and Methods B 268 18181823 ISSN 0168-583X 19th International Conference on Ion Beam Analysis
[15] Bogachev A. A. et al., 2021 Phys. Rev. C 104(2) 024623
[16] Viola V. E., Kwiatkowski K. and Walker M. 1985 Phys. Rev. C 31(4) 15501552
[17] Kozulin E. M. et al., 2022 Phys. Rev. C 105(1) 014607